

Crystal Structure of the Ordered Pyrochlore $\text{NH}_4\text{Fe}^{\text{II}}\text{Fe}^{\text{III}}\text{F}_6$ Structural Correlations with $\text{Fe}_2\text{F}_5 \cdot 2\text{H}_2\text{O}$ and Its Dehydration Product $\text{Fe}_2\text{F}_5 \cdot \text{H}_2\text{O}$

G. FERREY, M. LEBLANC, AND R. DE PAPE

Laboratoire des Fluorures et Oxyfluorures Ioniques (ERA-609), Faculté des Sciences, Route de Laval, 72017 Le Mans Cedex, France

Received March 26, 1979; in final form May 26, 1980

Crystal structure of $\text{NH}_4\text{Fe}^{\text{II}}\text{Fe}^{\text{III}}\text{F}_6$ is studied in order to explain further its peculiar antiferromagnetic behavior compared to the spin glass one of the pyrochlore family. $\text{NH}_4\text{Fe}^{\text{II}}\text{Fe}^{\text{III}}\text{F}_6$ is orthorhombic, space group $Pnma$ with $a = 7.045$ (4) Å, $b = 7.454$ (4) Å, $c = 10.116$ (6) Å, $Z = 4$. Diffraction data on single crystals obtained by hydrothermal synthesis, collected on an automatic four circle diffractometer, have been refined by full matrix least-squares calculations to a weighted value of 0.029 (unweighted $R = 0.024$) for 798 observed reflections. This structure is derived from the pyrochlore structure, with a cationic order between Fe^{2+} and Fe^{3+} ions. $(\text{Fe}^{\text{II}}\text{F}_6)^{4-}$ octahedra form infinite trans chains along [100] by sharing corners although similar chains of $(\text{Fe}^{\text{III}}\text{F}_6)^{3-}$ octahedra lie along [010]. This type of $\text{Fe}^{\text{II}}\text{-Fe}^{\text{III}}$ order is related to a similar one existing in $\text{Fe}_2\text{F}_5 \cdot 2\text{H}_2\text{O}$, the dehydration of which leads to the pyrochlore $\text{Fe}_2\text{F}_5 \cdot \text{H}_2\text{O}$. A mechanism is proposed to explain the formation of this compound.

Introduction

Fluorides containing two 3d transition metals exhibit two types of structural behavior which greatly influence the magnetic properties of the compounds; the 3d metallic cations are either ordered or randomly distributed in the structure (1-21).

Ordered structures occur in several structural types like MnCrF_5 (1-3), Cr_2F_5 (4), MnAlF_5 (5), NaMnCrF_6 (6, 7), $\text{A}_2\text{M}^{\text{II}}\text{M}'^{\text{III}}\text{F}_7$ weberites (8-10), $\text{A}_2\text{M}^{\text{II}}\text{M}'^{\text{I}}\text{F}_6$ elpasolites, cubic and hexagonal perovskites (11), and $\text{M}^{\text{II}}\text{M}'^{\text{I}}\text{F}_6$ compounds (12, 13) with LiSbF_6 structure (14).

On the contrary, $\text{LiM}^{\text{II}}\text{M}'^{\text{III}}\text{F}_6$ trirutiles (15, 16), hexagonal (17), tetragonal (17, 18) fluorobronzes, and $\text{AM}^{\text{II}}\text{M}'^{\text{III}}\text{F}_6$ pyrochlores (19-21) can generally be described

with a random distribution of divalent and trivalent 3d cations. In particular, this statistical repartition in the pyrochlore structure leads to a wide distribution of exchange interactions and a spin glass behavior (22, 23), studied on CsMnFeF_6 (24).

Nevertheless, order can occur in such compounds if the same metal exists in two valence states. The result is a lowering of the crystalline symmetry. It is the case for trirutile $\text{LiFe}^{\text{II}}\text{Fe}^{\text{III}}\text{F}_6$ (15, 16) and iron bronzes (1, 18, 19, 25, 28) and probably for vanadium (29) and chromium (30) bronzes. The cationic order has been precisely described in the stoichiometric compound $\text{K}_{0.6}\text{Fe}_{0.6}^{\text{II}}\text{Fe}_{0.4}^{\text{III}}\text{F}_6$ by X-ray diffraction and Mössbauer spectroscopy (1, 18, 25). In the case of $\text{A}^{\text{I}}\text{Fe}^{\text{II}}\text{Fe}^{\text{III}}\text{F}_6$ ($\text{A}^{\text{I}} = \text{Rb}^+, \text{Cs}^+, \text{Tl}^+$,

NH₄⁺) pyrochlores, the observed orthorhombic distortion also suggests Fe²⁺-Fe³⁺ ordering (19, 26-28).

In order to fix the type of cationic ordering in this last class of compounds and, further, to correlate it to the antiferromagnetic order opposed to the general spin glass behavior of disordered pyrochlores, we have studied the crystal structure of NH₄Fe^{II}Fe^{III}F₆ by X-ray diffraction. Our results are compared to cationic order occurring in Fe₂F₅ · 2H₂O, the dehydration of which leads to the pyrochlore Fe₂F₅ · H₂O. A mechanism is proposed to explain the formation of the monohydrate.

Experimental

Single crystals were grown by hydrofluorothermal synthesis, according to a method previously described (31, 51). The required quantities of iron fluorides were mixed with a 2 M NH₄HF₂ aqueous solution in a sealed platinum tube and introduced in an autoclave. The working conditions were as follows: 450°C—2350 bars. After 4 days, brown, well-shaped octahedral single crystals were obtained and characterized by their powder diffraction patterns (27) and Fe²⁺ and Fe³⁺ chemical analysis (Fe²⁺/Fe³⁺ = 1 ± 0.005) as NH₄Fe^{II}Fe^{III}F₆. Laue, Weissenberg, and precession photographs of crystal taken with MoK α radiation showed them to be orthorhombic with extinctions for *hkO* (*h* = 2*n*) and *Okl* (*k* + 1 = 2*n*) requiring the space group *Pnma*. The cell parameters, refined by a least-square procedure, and relevant crystal data are listed in Table I.

Intensity data were collected on a CAD 4 Nonius diffractometer¹ using MoK α radiation, in the range -9 ≤ *h* ≤ +9, -10 ≤ *k* ≤ +10, 0 ≤ *l* ≤ 14, with no restrictive conditions. Operating features were as fol-

¹ Inorganic Crystallochemistry Laboratory (Pr Hardy), Faculty of Sciences, Poitiers, France.

TABLE I
EXPERIMENTAL DATA FOR NH₄Fe^{II}Fe^{III}F₆ CRYSTALS

Symmetry: orthorhombic	Cell parameters: <i>a</i> = 7.045(4) Å
Space group: <i>Pnma</i> (<i>n</i> ² 62)	<i>b</i> = 7.454(4) Å
Conditions of <i>Okl</i> : <i>k</i> + <i>l</i> = 2 <i>n</i>	<i>c</i> = 10.116(6) Å
reflection <i>hkO</i> : <i>h</i> = 2 <i>n</i>	<i>z</i> = 4
$\rho_{\text{exp}} = 3.1 \text{ g/cm}^3$	Crystal dimension = 0.17 mm edge
$\rho_{\text{calc}} = 3.048 \text{ g/cm}^3$	$\mu \text{ (MoK}\alpha) = 53.8 \text{ cm}^{-1}$

lows: graphite monochromator; λ (MoK α) = 0.711 Å; 3° < θ < 30°; scan $\omega - 2\theta$; scan range *s* = 120 + 50 tg 2 θ in hundredth of degrees; scintillation counter aperture *D* = 20 + 2 tg θ in 10⁻¹ mm; scanning speed *v* = 20.1166/NV° mn⁻¹ with NV integer. The intensity treatment was realized using MAXE program (32). Only reflections with $\sigma(I)/I < 1$ were included in the refinement of the structure. $\sigma(I)/I$ has its usual significance: $\sigma(I)/I = \{I_M + 4(F_1 + F_2)/NV\}^{1/2}$ where *F*₁ and *F*₂ represents the background before and after reflection, and *I*_M the intensity of this reflection.

Structure Determination

The structure has been studied using the space group *Pnma*, the supplementary degrees of freedom obtained by considering the noncentrosymmetric group *Pn2₁a* giving no significant improvement of the results. A tridimensional Patterson map was calculated (MAXE program). Refinement by full matrix least-squares calculations was realized using a modified SFLS-5 program (33). The minimized function is $\sum \omega (|F_o| - Z_k |F_c|)^2$ where *F*_o and *F*_c are observed and calculated structure factors, *Z*_k a scale factor defined by $Z_k = \sum |F_o| / \sum |F_c|$ and ω the weighting. The Ibers weighting scheme, described in its final form by Grant *et al.* (34), has been used with *p* = 0.04 for $1/\omega = \sigma^2(F_o) = K \sigma(I)^2/4 LpI + p^2I$. Scattering factors for nitrogen, iron, and fluorine were calculated

using Vand's relation (35–37). The anomalous dispersion corrections $\Delta f'$ and $\Delta f''$ are taken from International Tables for X-Ray Crystallography (38).

The analysis of the Patterson map leads to localization of iron atoms in (4a) and (4c) sites of the $Pnma$ group. The refinement of the positional parameters of the (4c) site leads to an R value of 0.342. The coordinates of fluorine atoms were then determined using difference Fourier maps. The refinement of positional and isotropic thermal parameters of all atoms then gave an R factor 0.046 ($R_w = 0.055$), using during the two last cycles a secondary extinction factor of $7.37 \cdot 10^{-6}$. Refinement of anisotropic temperature factors reduced the residual to 0.024 ($R_w = 0.029$)², without any reject. The final positional and thermal parameters of nonhydrogen atoms are presented in Table II. Only a (8d) hydrogen position then appears on the difference Fourier map with approximate coordinates $x = 0.09$, $y = 0.13$, $z = 0.62$. The corresponding N–H bond would point toward F34. However, hydrogen atoms will be accurately localized by further neutron diffraction measurements.

Discussion of the Structure

Figure 1a presents the (001) projection of $\text{NH}_4\text{Fe}^{\text{II}}\text{Fe}^{\text{III}}\text{F}_6$. Its three-dimensional network derives from cubic pyrochlore by the relations $a_0 \approx b_0 \approx a_c/2^{1/2}$, $c_0 \approx c_c$ as can be seen when comparing to the corresponding

² See NAPS document No. 03647 for 7 pages of supplementary material. Order from ASIS/NAPS c/o Microfiche Publications, P. O. Box 3513, Grand Central Station, New York, New York 10017. Remit in advance for each NAPS Accession number. Institutions and organizations may use purchase orders when ordering, however, there is a billing charge for this service. Make checks payable to Microfiche Publications. Photocopies are \$5.00. Microfiche are \$3.00. Outside of the U.S. and Canada, postage is \$3.00 for a photocopy or \$1.50 for a fiche.

TABLE II
FINAL POSITIONAL AND ANISOTROPIC THERMAL PARAMETERS OF NONHYDROGEN ATOMS IN $\text{NH}_4\text{Fe}_2\text{F}_6$ ^{a,b}

Atom	Site	x	y	z	$\beta_{11} \cdot 10^4$	$\beta_{22} \cdot 10^4$	$\beta_{33} \cdot 10^4$	$\beta_{12} \cdot 10^4$	$\beta_{13} \cdot 10^4$	$\beta_{23} \cdot 10^4$	Beq
N	4c	0.0028(6)	1/4	0.6208(5)	129(7)	139(7)	44(3)	0	11(3)	0	2.49(12)
Fe ²⁺	4a	0	0	0	38(1)	17(1)	11(1)	-1(1)	2(1)	-3(1)	0.53(2)
Fe ²⁺	4c	0.2043(1)	1/4	0.2681(1)	33(1)	31(1)	14(1)	0	-2(1)	0	0.64(2)
F1	4c	-0.0627(2)	1/4	0.3398(1)	42(3)	106(3)	31(1)	0	-2(1)	0	1.50(5)
F2	4c	0.0633(2)	1/4	0.9671(2)	84(3)	25(2)	48(1)	0	14(2)	0	1.40(5)
F3	8d	0.1267(2)	0.4901(1)	0.1668(1)	106(2)	67(2)	21(1)	12(2)	-17(1)	3(1)	1.50(4)
F4	8d	0.7655(1)	0.4368(2)	0.0825(1)	62(2)	54(2)	35(1)	-3(1)	17(1)	13(1)	1.29(4)

^a Standard deviations are given in parentheses.

^b The vibrational coefficients relate to the expression $T = \exp -(\beta_{11}h^2 + \beta_{22}k^2 + \beta_{33}l^2 + 2\beta_{12}hk + 2\beta_{13}hl + 2\beta_{23}kl)$.

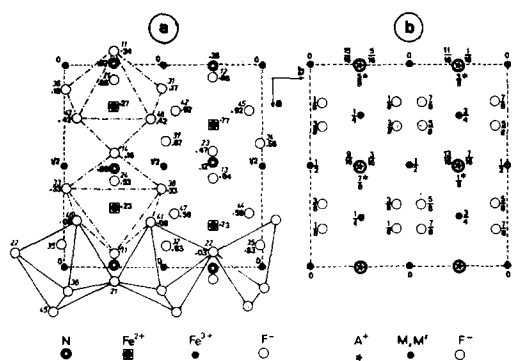


FIG. 1. (a) (001) projection of $\text{NH}_4\text{Fe}^{\text{II}}\text{Fe}^{\text{III}}\text{F}_6$. For fluorine atoms, numbers in italics correspond to the type and Wyckoff positions of atoms (see Table III); right numbers indicate z coordinates of F^- . (b) (001) projection of ideal pyrochlore $\text{AMM}'\text{F}_6$ in the same cell. The asterisks refer to z coordinate of A^+ ion.

projection (Fig. 1b) of a cubic pyrochlore such as RbNiCrF_6 (19, 20). From the observed bond distances (Table III), it is clear that iron (4a) sites are filled by Fe^{3+} ions while Fe^{2+} occupies (4c) sites. Such an order between Fe^{2+} and Fe^{3+} , predicted by Courbion (50), is consistent with previously described Mössbauer experiments (28). This order allows one to describe the structure as tilted trans chains of Fe^{2+} octahedra along [100] and of Fe^{3+} octahedra along [010] as can be seen on Fig. 1a. Each octahedron of Fe^{2+} and Fe^{3+} shares its six corners, thus giving the tridimensional structure. The Fe^{2+} ions are slightly displaced from their ideal coordinates, but the fluorine positions are very affected by the cationic order. The Fe^{2+} octahedra (Fig. 2) are very distorted with $\text{Fe}^{2+}\text{-F}^-$ distances varying from 1.973 to 2.134 Å (Table III), with an average bond length of 2.077 Å, slightly greater than the sum of Shannon's ionic radii (39) of hexacoordinated Fe^{2+} (0.780 Å) and of F^- with a coordination number of 2 (1.285 Å). The Fe^{3+} octahedron appears also in Fig. 2 with the thermal vibration ellipsoids; it is quite regular. The average bond length is 1.923 Å, close to the sum of Fe^{3+} and F^- radii (1.930 Å). With

comparison to the ideal 18 coordination of A^+ , only 13 fluorine atoms surround nitrogen (Table III). The N-F distances vary between 2.885 and 3.772 Å, with an average value of 3.236 Å.

Structural Correlations

Such a type of $\text{Fe}^{2+}\text{-Fe}^{3+}$ order was recently described for the ferrimagnetic hydrated mixed valence iron fluoride $\text{Fe}_2\text{Fe}_5 \cdot 2\text{H}_2\text{O}$ (40) previously studied by several authors (41-47). This compound is also orthorhombic (*Imma*). As in $\text{NH}_4\text{Fe}^{\text{II}}\text{Fe}^{\text{III}}\text{F}_6$, trans chains of $\text{Fe}^{\text{III}}\text{F}_6$ octahedra are observed, but the $\text{Fe}^{\text{II}}\text{F}_4(\text{H}_2\text{O})_2$ octahedra are not connected together (Fig. 3); the aquo groups are terminal, and the $\text{Fe}^{\text{II}}\text{F}_4(\text{H}_2\text{O})_2$ polyhedra share only their four equatorial fluorine atoms with two iron III chains.

The dehydration of $\text{Fe}_2\text{F}_5 \cdot 2\text{H}_2\text{O}$ has been simultaneously studied by Gallagher and Ottaway (45) and Charpin and Mache-teau (44). It leads to intermediate products, successively B and a mixture of a new

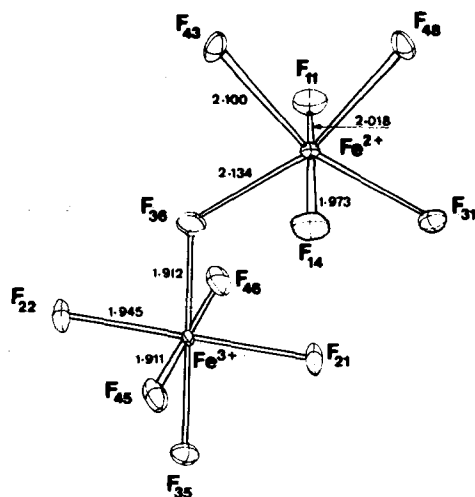


FIG. 2. Coordination polyhedra with distances and anisotropic thermal vibration ellipsoids of Fe^{2+} (symmetry m) and Fe^{3+} (symmetry l). Symbols of fluorine atoms refer to Table III. They correspond to (001) projection of Fig. 1a.

TABLE III
INTERATOMIC DISTANCES, POLYHEDRAL EDGE LENGTHS, AND BOND ANGLES^a

Octahedron of Fe^{3+} (0, 0, 0)(center of symmetry)			
Fe-F21	1.945(1)	F21-F36	2.736(3)
Fe-F36	1.912(1)	F21-F45	2.670(3)
Fe-F45	1.911(1)	F21-F35	2.718(3)
		F21-F46	2.751(3)
F21-Fe-F45	87.88(10)	F36-F45	2.691(3)
F21-Fe-F36	90.38(11)	F36-F46	2.716(3)
F36-Fe-F45	89.47(10)		
Octahedron of Fe^{2+} (0.204, 1/4, 0.268) symmetry <i>m</i>			
Fe-F11	2.018(1)	F11-F36	2.837(5)
Fe-F14	1.973(1)	F11-F43	2.814(5)
Fe-F36	2.134(2)	F14-F36	2.830(5)
Fe-F43	2.100(2)	F14-F43	3.191(7)
		F36-F43	2.746(4)
		F36-F31	3.580(8)
		F43-F48	2.785(4)
F11-Fe-F36	86.17(10)	F36-Fe-F43	80.89(9)
F11-Fe-F43	86.18(10)	F36-Fe-F31	114.05(13)
F14-Fe-F36	87.01(10)	F43-Fe-F48	83.10(9)
F14-Fe-F43	103.12(13)		
Surrounding of N (0.0028, 1/4, 0.6208) symmetry <i>m</i>			
N-F34	3.285(7)	2 × N-F12	3.772(9)
N-F37	3.285(7)	N-F32	3.030(6)
N-F43	3.102(6)	N-F35	3.030(6)
N-F48	3.102(6)	N-F44	3.031(6)
N-F21	3.525(8)	N-F47	3.031(6)
N-F11	2.885(5)	N-F24	3.226(7)

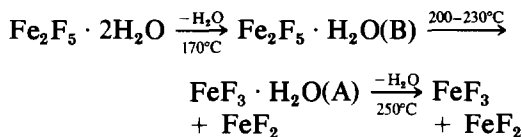
^a Fluorine ions are noted by two numbers: the first refers to the type of fluoride designed in Table II, the second characterizes the Wyckoff position noted as follows:

8d sites (1) $x y z$ (3) $\frac{1}{2} + x \frac{1}{2} - y \frac{1}{2} - z$ (5) $\bar{x} \frac{1}{2} + y \bar{z}$ (7) $\frac{1}{2} - x \bar{y} \frac{1}{2} + z$
(F3-F4) (2) $\bar{x} \bar{y} \bar{z}$ (4) $\frac{1}{2} - x \frac{1}{2} + y \frac{1}{2} + z$ (6) $x \frac{1}{2} - y z$ (8) $\frac{1}{2} + x y \frac{1}{2} - z$

4c sites (1) $x \frac{1}{4} z$ (2) $\bar{x} \frac{3}{4} \bar{z}$ (3) $\frac{1}{2} - x, \frac{3}{4}, \frac{1}{2} + z$ (4) $\frac{1}{2} + x \frac{1}{4} \frac{1}{2} - z$
(F1-F2)

product A with FeF_2 ; A and B are considered as anhydrous products by Gallagher. The B species was found to be $\text{Fe}_2\text{F}_5 \cdot \text{H}_2\text{O}$ by Charpin and Macheteau (44) by T.G.A. measurements. The A product was previously identified (48) as $\text{FeF}_3 \cdot \text{H}_2\text{O}$ by chemical analysis. We prepared single crystals of this compound by hydrothermal synthesis (31) and showed its analogy with the hexagonal tungsten bronze structure (49);

the presence of water was confirmed by ir measurements. The thermal decomposition scheme, proposed by Charpin and Macheteau (44)



agrees with all these results.

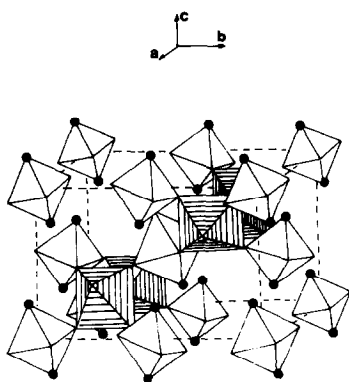


FIG. 3. Perspective view of $\text{Fe}_2\text{F}_5 \cdot 2\text{H}_2\text{O}$ structure. H_2O molecules are drawn as black circles. Iron(III) octahedra are shaded.

This scheme implies that B is hydrated. Its X-ray pattern was indexed like a cubic pyrochlore: $a = 10.353 (2) \text{ \AA}$. Then the formula $\text{Fe}_2\text{F}_5 \cdot \text{H}_2\text{O}$ is consistent with the fact that a B_2X_6 ($X = \text{F}, \text{H}_2\text{O}$) skeleton is necessary for the existence of such a structure in which FeX_6 octahedra share all their vertices, giving a structural formula

$\text{Fe}^{\text{II}}\text{X}_{6/2}\text{Fe}^{\text{III}}\text{X}_{6/2}$ (20, 21). If the structures of $\text{Fe}_2\text{F}_5 \cdot 2\text{H}_2\text{O}$ and $\text{NH}_4\text{Fe}^{\text{II}}\text{Fe}^{\text{III}}\text{F}_6$ are considered, it appears that the formation of pyrochlore type monohydrate $\text{Fe}_2\text{F}_5 \cdot \text{H}_2\text{O}$ can be explained by the cooperative elimination of one H_2O molecule between two $\text{Fe}^{\text{II}}\text{F}_4(\text{H}_2\text{O})_2$ octahedra as described by arrows in Fig. 4. Such a simplistic mechanism would keep $\text{Fe}^{\text{II}}\text{-Fe}^{\text{III}}$ order in the monohydrate and consequently lead to a noncubic pyrochlore. Its structural formula would be $\text{Fe}^{\text{II}}\text{F}_{4/2}(\text{H}_2\text{O})_{2/2}\text{Fe}^{\text{III}}\text{F}_{6/2}$. The true mechanism is probably more complicated because no deformation of the pyrochlore structure has been observed by Charpin and Gallagher (44, 45).

It was important to solve the structure of $\text{NH}_4\text{Fe}^{\text{II}}\text{Fe}^{\text{III}}\text{F}_6$ in order to explain its peculiar antiferromagnetic behavior, compared to the spin glass one observed for CsMnFeF_6 pyrochlore in which divalent and trivalent ions are statistically distributed. A complete magnetic study of this compound is now possible and will soon begin in Laue Langevin Institute in Grenoble.

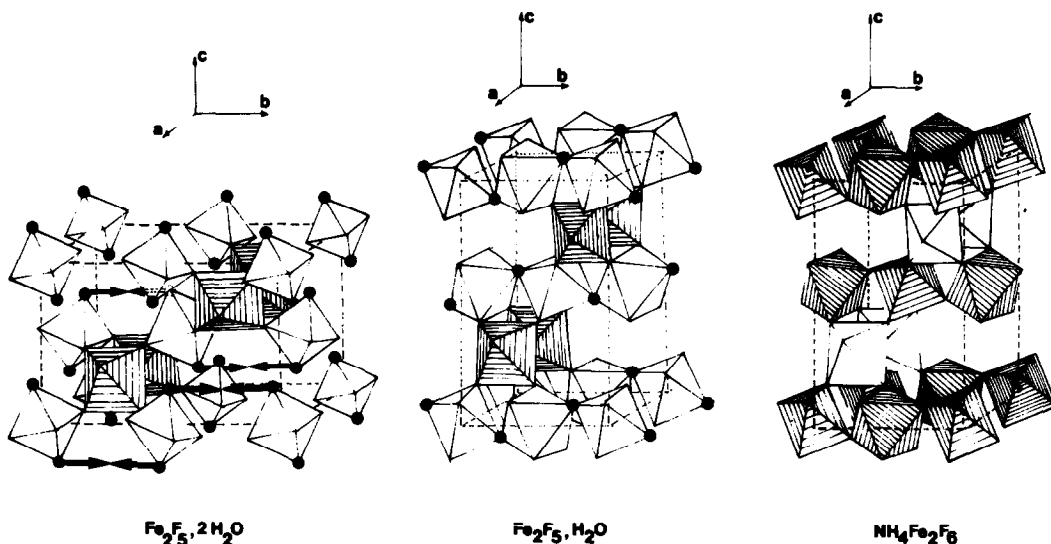


FIG. 4. Proposed mechanism of cooperative elimination of H_2O molecules (arrows) during the dehydration of $\text{Fe}_2\text{F}_5 \cdot 2\text{H}_2\text{O}$ leading to pyrochlore-type $\text{Fe}_2\text{F}_5 \cdot \text{H}_2\text{O}$ compared to $\text{NH}_4\text{Fe}^{\text{II}}\text{Fe}^{\text{III}}\text{F}_6$. Iron(III) octahedra are shaded.

Acknowledgments

The authors are grateful to Dr. G. Courbion for helpful discussions in the derivation of subgroups of $Fd3m$ pyrochlore that he had previously described (50), to Dr. J. Pannetier for helpful discussions, and to Pr. A. Hardy and Dr. A. M. Hardy for providing us with all facilities for data collections.

References

- G. FERÉY, Thèse de Doctorat d'Etat Paris VI (1977).
- G. FERÉY, R. DE PAPE, M. POULAIN, D. GRANDJEAN, AND A. HARDY, *Acta Crystallogr. B* **33**, 1409 (1977).
- G. FERÉY, R. DE PAPE, AND B. BOUCHER, *Acta Crystallogr. B* **34**, 1084 (1978).
- H. STEINFINK AND J. M. BURNS, *Acta Crystallogr.* **17**, 823 (1964).
- A. RIMSKY, J. THORET, AND W. FREUNDLICH, *C. R. Acad. Sci.* **270C**, 407 (1970).
- G. COURBION, C. JACOBONI, AND R. DE PAPE, *Acta Crystallogr. B* **33**, 1405 (1977).
- G. COURBION, G. FERÉY, AND R. DE PAPE, *Mat. Res. Bull.* **13**, 967 (1978).
- G. COURBION, personal communication.
- R. HAEGELE, W. VERSCHAAREN, D. BABEL, J. M. DANCE, AND A. TRESSAUD, *J. Solid State Chem.* **24**, 77 (1978).
- W. VERSCHAAREN AND D. BABEL, *J. Solid State Chem.* **24**, 405 (1978).
- J. M. DANCE AND A. TRESSAUD, "Advances in Inorganic Chemistry," Vol. 20, p. 133. Academic Press, New York (1977).
- H. HENKEL AND R. HOPPE, *Z. Anorg. Allgem. Chem.* **359**, 160 (1968).
- A. TRESSAUD, M. WINTERBERGER, N. BARTLETT, AND P. HAGENMULLER, *C.R. Acad. Sci.* **282C**, 1069 (1976).
- J. H. BURNS, *Acta Crystallogr.* **15**, 1098 (1962).
- N. N. GREENWOOD, A. T. HOWE, AND F. MENIL, *J. Chem. Soc. A* 2218 (1971).
- F. MENIL, Thèse de Doctorat d'Etat Bordeaux (1973).
- R. DE PAPE, *C.R. Acad. Sci.* **260**, 4527 (1965).
- A. M. HARDY, A. HARDY, AND G. FERÉY, *Acta Crystallogr. B* **29**, 1654 (1979).
- D. BABEL, G. PAUSEWANG, AND W. VIEBAHN, *Z. Naturforsch.* **22b**, 1219 (1967).
- D. BABEL, *Z. Anorg. Allgem. Chem.* **387**, 161 (1972).
- C. JACOBONI, Thèse de Doctorat d'Etat Paris VI (1975).
- W. KURTZ, Dissertation Tübingen (1977).
- S. ROTH AND W. KURTZ, *Physica* **86-88 B**, 715 (1977).
- J. VILLAIN, *Z. Phys. B* **33**, 31 (1979).
- G. FERÉY, R. DE PAPE, AND F. VARRET, *J. Phys. C7* **38**, 107 (1977).
- A. TRESSAUD, R. DE PAPE, AND J. PORTIER, *C.R. Acad. Sci.* **270**, 726 (1970).
- A. TRESSAUD, R. DE PAPE, J. PORTIER, AND P. HAGENMULLER, *Bull. Soc. Chim. Fr.* 3411 (1970).
- N. N. GREENWOOD, F. MENIL, AND A. TRESSAUD, *J. Solid State Chem.* **5**, 402 (1972).
- C. CROS, R. FEURER, AND M. POUCHARD, *Mat. Res. Bull.* **10**, 383 (1975).
- D. DUMORA, Thèse de Doctorat d'Etat Bordeaux (1971).
- G. FERÉY, M. LEBLANC, R. DE PAPE, AND M. PASSARET, AND M. BOTHOREL-RAZAZI, *J. Crystal Growth* **29**, 209 (1975).
- J. Y. LE MAROUILLE, Thèse de 3ème Cycle Rennes (1972).
- C. T. PREWITT, SFLS.5: A Fortran IV Full Matrix Crystallographic Least Squares Program (1966).
- D. F. GRANT, R. C. G. KILLEAN, AND J. L. LAWRENCE, *Acta Crystallogr. B* **25**, 374 (1969).
- V. VAND, P. F. EILAND, AND R. PEPINSKY, *Acta Crystallogr.* **10**, 303 (1957).
- J. B. FORSYTH AND M. WELLS, *Acta Crystallogr.* **12**, 412 (1959).
- F. H. MOORE, *Acta Crystallogr.* **16**, 1169 (1963).
- "International Tables for X-ray Crystallography," Vol. IV. Kynoch Press, Birmingham (1968).
- R. D. SHANNON, *Acta Crystallogr. A* **32**, 751 (1976).
- W. HALL, S. KIM, J. ZUBIETA, E. G. WALTON, AND D. B. BROWN, *Inorg. Chem.* **16**, 1884 (1977).
- E. G. WALTON, D. B. BROWN, H. WONG, AND W. M. REIFF, *Inorg. Chem.* **16**, 2425 (1977).
- G. BRAUER AND M. EICHNER, *Z. Anorg. Allgem. Chem.* **296**, 13 (1958).
- T. SAKAI AND T. TOMINAGA, *Radioisotopes* **23**, 347 (1974).
- P. CHARPIN AND Y. MACHETEAU, *C.R. Acad. Sci.* **280C**, 61 (1975).
- K. J. GALLAGHER AND M. R. OTTAWAY, *J. Chem. Soc. Dalton Trans.* 978 (1975).
- P. IMBERT, G. JEHANNO, Y. MACHETEAU, AND F. VARRET, *J. Phys. (Paris)* **37**, 969 (1976).
- K. J. GALLAGHER AND M. R. OTTAWAY, *J. Chem. Soc. Dalton Trans.* 2212 (1977).
- Y. MACHETEAU AND P. CHARPIN, *C.R. Acad. Sci.* **275C**, 443 (1972).
- A. MAGNELI, *Acta Chem. Scand.* **7**, 315 (1953).
- G. COURBION, Thèse de 3ème Cycle Rennes (1974).
- F. PLET, J. L. FOURQUET, G. COURBION, M. LEBLANC, AND R. DE PAPE, *J. Crystal Growth* **47**, 699 (1979).